UDC 621.317 https://doi.org/10.20998/2074-272X.2026.1.04

A. Bounab, A. Chaiba, S. Belkacem, A. Chariete

Performance improvement of parallel dual-star permanent magnet synchronous machines via type-2 fuzzy direct torque control with a single six-phase inverter

Introduction. *The growing need for efficient and high-performance electric drive systems has led to increased research in advanced control strategies for multi-machine configurations. Among them, dual-star permanent magnet synchronous machines (DSPMSMs) connected in parallel to a single inverter offer a promising solution for applications requiring high reliability and precise control.* ***Problem.*** *Conventional direct torque control (DTC) strategies, typically relying on PI controllers, suffer from significant torque and flux ripples, which negatively impact system efficiency and dynamic response. Moreover, these traditional controllers face challenges in handling parameter variations and external disturbances, limiting their applicability in demanding environments.* ***Goal.*** *This study aims to enhance the performance of DSPMSM drive systems by improving speed regulation, minimizing torque and flux fluctuations, and increasing robustness against disturbances, thereby ensuring greater efficiency and stability.* ***Methodology.*** *To address these challenges, we propose a novel DTC strategy that replaces the conventional PI controller with a type-2 fuzzy logic controller (T2-FLC). This intelligent control approach leverages the adaptability of fuzzy logic to improve response accuracy and dynamic performance. The proposed methodology is validated through extensive simulations using MATLAB/Simulink, analyzing various operating conditions and comparing the performance with conventional DTC techniques.* ***Results.*** *Simulation results confirm that the T2-FLC-based DTC significantly reduces torque and flux ripples while ensuring precise speed regulation. The proposed approach also demonstrates improved robustness against disturbances and parameter variations, outperforming traditional PI-based DTC in terms of efficiency and control accuracy.* ***Scientific novelty****. This research introduces an innovative application of T2-FLC in DTC for parallel-connected DSPMSMs, offering a novel control strategy that effectively mitigates the drawbacks of conventional methods. The integration of T2-FLC into the DTC framework provides enhanced adaptability and superior performance, distinguishing this study from existing works.* ***Practical value.*** *The proposed control strategy enhances the reliability, efficiency, and stability of DSPMSM-based drive systems, making it well-suited for high-performance applications such as railway traction, electric vehicles, and industrial automation. By improving control precision and robustness, this approach contributes to the advancement of intelligent drive technologies in modern electric propulsion systems.* References 39, tables 4, figures 16.

Key words: **permanent magnet synchronous machine, type-2 fuzzy logic controller, direct torque control, six-phase inverter, multi-machines system.**

Вступ*. Зростаюча потреба в ефективних та високопродуктивних системах електроприводу призвела до посилення досліджень удосконалених стратегій керування для багатомашинних конфігурацій. Серед них, синхронні машини з постійними магнітами та обмоткою статора за схемою з'єднання «зірка» із спільним регулюванням струмів обмоток статора (DSPMSM), що підключені паралельно до одного інвертора, пропонують перспективне рішення для застосувань, які вимагають високої надійності та точного керування.* ***Проблема****. Традиційні стратегії прямого керування крутним моментом (DTC), які базуються на PI-контролерах, мають значні пульсації крутного моменту та потоку, що негативно впливає на ефективність системи та динамічну характеристику. Крім того, ці традиційні контролери стикаються з проблемами обробки коливань параметрів та зовнішніх збурень, що обмежує їхню застосовність у складних умовах.* ***Мета****. Це дослідження спрямоване на підвищення продуктивності систем приводу DSPMSM шляхом покращення регулювання швидкості, мінімізації коливань крутного моменту та потоку, а також підвищення стійкості до збурень, тим самим забезпечуючи більшу ефективність та стабільність.* ***Методологія****. Для вирішення цих проблем запропоновано нову стратегію DTC, яка замінює традиційний PI-контролер контролером з нечіткою логікою 2-го типу (T2-FLC). Цей інтелектуальний підхід до керування використовує адаптивність нечіткої логіки для покращення точності відгуку та динамічних характеристик. Запропонована методологія перевірена за допомогою масштабної симуляції з використанням MATLAB/Simulink, аналізуючи різні робочі умови та порівнюючи продуктивність з традиційними DTC методам.* ***Результати*** *моделювання підтверджують, що DTC на основі T2-FLC значно зменшує пульсації крутного моменту та потоку, забезпечуючи при цьому точне регулювання швидкості. Запропонований підхід демонструє покращену стійкість до збурень та коливань параметрів, перевершуючи традиційний DTC на основі PI з точки зору ефективності та точності керування.* ***Наукова новизна****. Це дослідження представляє інноваційне застосування T2-FLC у DTC для паралельно з'єднаних DSPMSM, пропонуючи нову стратегію керування, яка ефективно усуває недоліки звичайних методів. Інтеграція T2-FLC у структуру DTC забезпечує покращену адаптивність та високу продуктивність, що відрізняє це дослідження від існуючих робіт.* ***Практична значимість****. Запропонована стратегія керування підвищує надійність, ефективність та стабільність систем приводу на основі DSPMSM, що робить її добре придатною для високопродуктивних застосувань, таких як залізниця, електромобілі та промислова автоматизація. Завдяки покращенню точності та надійності керування, цей підхід сприяє розвитку інтелектуальних технологій приводу в сучасних електричних рушійних системах.* Бібл. 39, табл. 4, рис. 16.

Ключові слова: **синхронна машина з постійними магнітами, контролер з нечіткою логікою 2 типу, пряме управління крутним моментом, шестифазний інвертор, багатомашинна система.**

Introduction. In today's rapidly evolving industrial landscape, there is an increasing focus on optimizing system performance while reducing weight, volume, and operating costs. To achieve this ambitious goal, the concept of using a multi-machine drive system powered by a single inverter has emerged as an innovative solution. Such systems find applications in various industries, including paper and rolling mills, transportation, electric traction, marine propulsion, and electric vehicles.

In the domain of multi-motor drives, the design and control strategy of the drive system must be carefully tailored to meet the specific requirements of the application. These include factors such as output power, speed control, and accuracy [1–8]. The implementation of drive techniques involving the parallel connection of two dual-star permanent magnet synchronous machines (DSPMSMs), both powered by a six-phase pulse width modulation (PWM) inverter, has been adopted in various

industrial applications [1, 2, 9]. However, when it comes to controlling the speed of multi-phase drives, traditional control mechanisms face persistent challenges due to parameter variations, flux and torque ripples, and the effects of power disturbances on the load [9–11].

To address these issues, this paper proposes an innovative approach [12] by integrating a type-2 fuzzy logic controller (T2-FLC) with direct torque control (DTC) to regulate the speed of two DSPMSMs operating in parallel [13–15]. This method not only improves system performance but also mitigates torque and flux ripples that could otherwise affect operational efficiency. The motivation behind this work lies in overcoming the limitations of traditional DTC methods [9–11], which are known for their sensitivity to rotor parameter variations and challenges in managing variable switching frequencies due to the use of hysteresis controllers [12].

In response, this work explores a state-of-the-art methodology by integrating a T2-FLC, aiming to overcome these limitations and provide a more suitable approach for systems affected by uncertainty.

Extensive research on the application of type-2 fuzzy logic in engineering is ongoing, highlighting several advantages over type-1 fuzzy logic controller (T1-FLC) in systems affected by uncertainty [15–19]. Recent studies confirm that the T2-FLC offers better performance than T1-FLC in managing uncertain or imprecise system parameters [20–22].

Before presenting the proposed methodology, it is important to review the current state of the art. DSPMSMs, featuring two star-connected three-phase stator windings shifted by 30°, offer several advantages over conventional three-phase PMSMs. These include lower torque ripple, reduced current harmonics, higher reliability, and greater power capability [23]. Moreover, DTC has proven effective in achieving high dynamic performance in AC motor drives [24]. Traditional DTC methods estimate torque and flux to select appropriate voltage vectors, keeping errors within hysteresis bands. While this enables fast torque response, it results in variable switching frequencies [25].

Fuzzy logic controller (FLC) provides an alternative control strategy that relies on linguistic rules and membership functions (MFs) rather than complex mathematical models [26]. FLC is recognized for its robustness against uncertainties and is particularly well-suited for complex, nonlinear systems. T2-FLCs are distinguished by their ability to handle higher degrees of uncertainty compared to T1-FLCs [27].

Recent studies have investigated the integration of intelligent control techniques to enhance the performance of DTC. Notable developments include fuzzy-based DTC strategies for induction motors, which have demonstrated improved speed regulation and reduced maintenance costs [1]. Fuzzy logic controllers have also been incorporated into DTC systems to improve the efficiency, reliability, and dynamic behavior of variable-speed drives in a wide range of applications. For example, fuzzy-2 DTC combined with space vector pulse width modulation has shown faster dynamic responses, lower total harmonic distortion (THD) in current and voltage, and reduced capacitor voltage spikes in induction motor drives, outperforming conventional PI-DTC schemes [24].

Furthermore, FLCs have been applied to DTC schemes to improve the overall performance of variable-speed drive systems. In [25], a fractional-order FLC was introduced to enhance the dynamic performance of DTC in induction motors, leading to significant gains in efficiency and reliability. In [27], FLC was employed to optimize electromagnetic torque and speed regulation in induction machines, effectively replacing conventional hysteresis comparators and PI speed controllers.

Additionally, DTC has been integrated with adaptive fuzzy control in the case of DSPMSMs, significantly reducing harmonic currents and improving efficiency in high-power traction applications [28]. Fuzzy logic-based control has also been applied to grid-connected photovoltaic inverters, stabilizing output voltage and current, minimizing THD, and enabling power injection into the grid when generation exceeds local demand [29].

In PMSMs, fuzzy logic-based DTC techniques have enabled the reduction of torque and flux ripples without modifying the inverter's switching frequency [30]. Moreover, fuzzy logic has been used for the control of DSPMSMs connected in parallel and supplied by a single six-phase inverter, achieving superior speed tracking performance, particularly under load disturbances [15].

In the context of five-phase interior PMSMs, a fuzzy logic-based DTC space vector modulation approach was proposed, offering fast and simple speed control while outperforming classical DTC methods [18].

In this paper, we propose an innovative speed control approach for DSPMSMs operating in parallel and supplied by a single six-phase PWM inverter. Our contribution lies in the integration of a T2-FLC with DTC to address the complex challenges of multi-motor control. The use of a six-phase PWM inverter, as emphasized in this work, enhances both system reliability and overall performance compared to traditional configurations.

The integration of T2-FLC plays a crucial role in addressing elevated levels of uncertainty, which are often encountered in real-world applications. Combined with DTC, well known for its high dynamic performance in AC motor drives, the proposed approach yields an intelligent and adaptive control strategy that significantly improves system behavior under varying operating conditions. This research highlights the advantages of T2-FLC over its T1-FLC counterpart, particularly in scenarios where uncertainty is a dominant factor, thus demonstrating the practical relevance of T2-FLC implementation in industrial contexts. In summary, the proposed method constitutes a significant advancement in motor drive control, with the potential to enhance the reliability, efficiency, and overall performance of electric drive systems across a wide range of applications.

The goal of the work is to enhance the performance of DSPMSM drive systems by improving speed regulation, minimizing torque and flux fluctuations, and increasing robustness against disturbances, thereby ensuring greater efficiency and stability. Unlike conventional DTC approaches that rely on PI controllers and suffer from significant torque and flux ripples, the proposed method introduces an adaptive and intelligent control scheme that improves dynamic response, minimizes electromagnetic ripples, and ensures stable operation under parameter uncertainties and external disturbances.

System configuration. Figure 1 shows the configuration of the proposed DTC system applied to two DSPMSMs operating in parallel and driven by a single six-phase inverter. This topology effectively mitigates the risk of over-magnetization in the machines, preserving performance and system integrity.

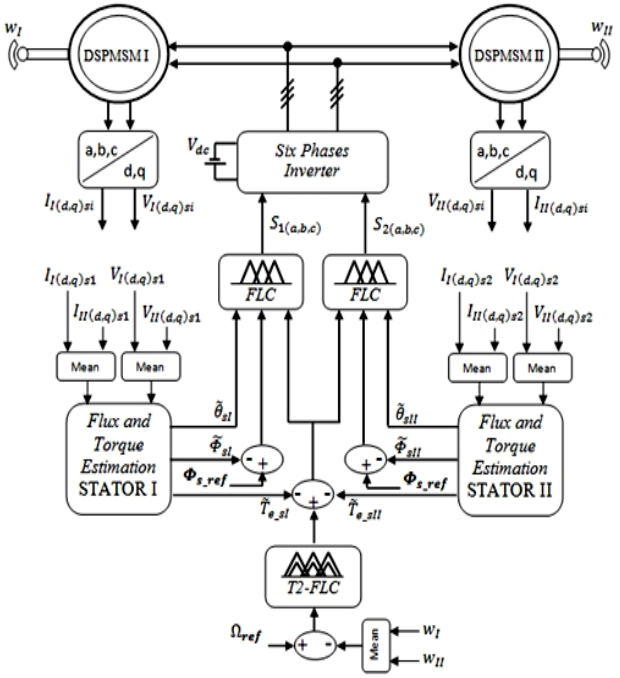

Fig. 1. Block diagram of the type-2 fuzzy logic-based DTC for two DSPMSMs

The core principle of DTC lies in determining the appropriate switching states of the voltage source inverter to directly control the stator voltage vectors. The selection of these vectors is based on a predefined switching table that considers torque and flux errors, along with the position of the stator flux vector. This process is critical to achieving accurate control and optimizing the overall performance of the drive system.

The rotational speed of both machines is measured using high-precision sensors, enabling fine speed regulation. To achieve this level of control accuracy, the T2-FLC is embedded within the outer speed regulation loop of the DSPMSM drive, as shown in Fig. 1.

Additionally, the system's capability to handle a wide range of disturbances is thoroughly evaluated. These disturbances include internal factors such as parameter variations, as well as external influences such as load changes and speed fluctuations. This comprehensive analysis demonstrates the system's ability to maintain stable and reliable performance, even under dynamic and uncertain operating conditions. This aspect reflects the scientific rigor and practical relevance of the proposed approach.

DSPMSM model. A comprehensive mathematical model is developed to represent the dynamic behavior of the DSPMSM. The state variables include stator currents, stator flux components, and rotor speed, while the control inputs are the stator voltages (V_{ds}, V_{qs}). The model is formulated in the (d–q) reference frame, which rotates synchronously with the rotor magnetic field. The dynamic behavior is expressed through a set of differential equations (1–4) [31, 32]:

$$\begin{cases} V_{ds1,i}=R_{s1,i}\cdot I_{ds1,i}+\dfrac{\mathrm{d}\Phi_{ds1,i}}{\mathrm{d}t}-w_{si}\cdot\Phi_{qs1,i};\\ V_{qs1,i}=R_{s1,i}\cdot I_{qs1,i}+\dfrac{\mathrm{d}\Phi_{qs1,i}}{\mathrm{d}t}-w_{si}\cdot\Phi_{ds1,i};\\ V_{ds2,i}=R_{s2,i}\cdot I_{ds2,i}+\dfrac{\mathrm{d}\Phi_{ds2,i}}{\mathrm{d}t}-w_{si}\cdot\Phi_{qs2,i};\\ V_{qs2,i}=R_{s2,i}\cdot I_{qs2,i}+\dfrac{\mathrm{d}\Phi_{qs2,i}}{\mathrm{d}t}-w_{si}\cdot\Phi_{ds2,i}, \end{cases} \quad (1)$$

where the expressions of stators fluxes are:

$$\begin{cases} \Phi_{ds1,i}=L_{ds1,i}\cdot I_{ds1,i}+M_{ds2,i}\cdot I_{ds2,i}+\Phi_{PM,i};\\ \Phi_{qs1,i}=L_{qs1,i}\cdot I_{qs1,i}+M_{qs2,i}\cdot I_{qs2,i};\\ \Phi_{ds2,i}=L_{ds2,i}\cdot I_{ds2,i}+M_{ds1,i}\cdot I_{ds1,i}+\Phi_{PM,i};\\ \Phi_{qs2,i}=L_{qs2,i}\cdot I_{qs2,i}+M_{qs1,i}\cdot I_{qs1,i}. \end{cases} \quad (2)$$

In these equations, the subscripts (s_1, s_2) designate the 1st and 2nd stator of both DSPMSMs, while subscripts (i = 1, 2) denote variables and parameters about DSPSM1 and DSPSM2, respectively. The variables and parameters include: [($V_{ds1,i}$, $V_{qs1,i}$,), ($V_{ds2,i}$, $V_{qs2,i}$)]; [($I_{ds1,i}$, $I_{qs1,i}$,), ($I_{ds2,i}$, $I_{qs2,i}$)]; [($\Phi_{ds1,i}$, $\Phi_{qs1,i}$,), ($\Phi_{ds2,i}$, $\Phi_{qs2,i}$)]; [($L_{ds1,i}$, $L_{qs1,i}$,), ($L_{ds2,i}$, $L_{qs2,i}$)]; [($M_{ds1,i}$, $M_{qs1,i}$,), ($M_{ds2,i}$, $M_{qs2,i}$)] and $\Phi_{PM,i}$, representing voltage, currents, stator flux linkage, stator inductance, mutual inductance in the (d–q) axis, and the permanent magnet flux, respectively.

The mechanical equation of the machine is:

$$J_i\frac{\mathrm{d}\Omega_i}{\mathrm{d}t}+fr_i\cdot\Omega_i=T_{e_i}-T_{r_i}, \quad (3)$$

where J is the moment of inertia; fr is the friction coefficient; T_e is the electromagnetic torque; T_r is the load torque; Ω is the rotor's mechanical speed [13].

The structural representation of the DSPMSM in the electrical domain is depicted in Fig. 2.

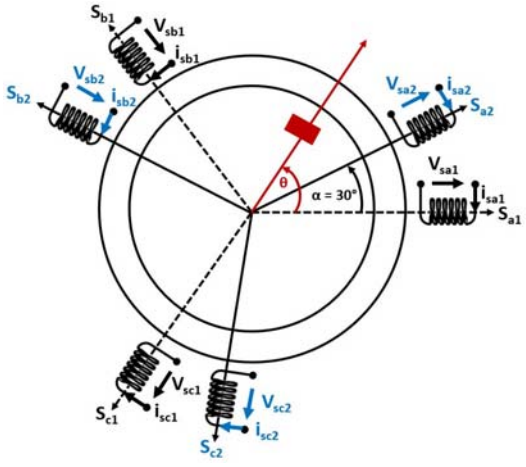

Fig. 2. Schematic of the DSPMSM stator windings

The electromagnetic torque equation is articulated in terms of stator currents and stator flux as:

$$T_{e_i}=p\cdot\begin{pmatrix}\Phi_{ds1,i}\cdot I_{qs1,i}-\Phi_{qs1,i}\cdot I_{ds1,i}+\\ +\Phi_{ds2,i}\cdot I_{qs2,i}-\Phi_{qs2,i}\cdot I_{ds2,i}\end{pmatrix}, \quad (4)$$

where p is the number of pole pairs.

Six-phase inverter model. The stator windings of the DSPMSMs are supplied by a six-phase voltage source inverter, as shown in Fig. 3 [33]. In this configuration, the

notation K_{a1}, K_{b1}, K_{c1} represent the switches of the upper half-bridge, while K_{a2}, K_{b2}, K_{c2} correspond to the switches of the lower half-bridge. Additionally, n_1 and n_2 denote the neutral points associated with stator 1 and stator 2, respectively.

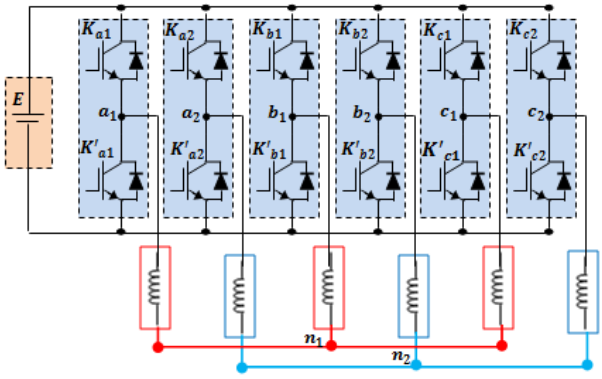

Fig. 3. Schematic diagram of the six-phase inverter

It is important to note that, since the windings of stator 1 and stator 2 are assumed to be ideally balanced and their neutral points are not connected, the phase voltages do not contain any zero-sequence components. As a result, equation (5) remains valid under these conditions:

$$\begin{aligned} V_{sa1}+V_{sb1}+V_{sc1}&=0;\\ V_{sa2}+V_{sb2}+V_{sc2}&=0. \end{aligned} \tag{5}$$

Furthermore, equation (6) accurately represents the voltage vector generated by the six-phase inverter:

$$\begin{bmatrix} V_{sa1}\\ V_{sb1}\\ V_{sc1}\\ V_{sa2}\\ V_{sb2}\\ V_{sc2} \end{bmatrix} = \begin{bmatrix} 2 & -1 & -1 & 0 & 0 & 0\\ -1 & 2 & -1 & 0 & 0 & 0\\ -1 & -1 & 2 & 0 & 0 & 0\\ 0 & 0 & 0 & 2 & -1 & -1\\ 0 & 0 & 0 & -1 & 2 & -1\\ 0 & 0 & 0 & -1 & -1 & 2 \end{bmatrix} \begin{bmatrix} V_{a10}\\ V_{b10}\\ V_{c10}\\ V_{a20}\\ V_{b20}\\ V_{c20} \end{bmatrix}. \tag{6}$$

When multiple motors are connected in parallel and supplied by a single inverter, the inverter directly controls the current to ensure proper system operation. However, discrepancies in speed or parameter variations between the two motors can lead to an imbalance in the currents flowing through each stator winding. The stator currents $I_{s1,i}$ and $I_{s2,i}$ are flowing in each machine, can be represented by $I_{s,i}$ which flows equally in both stators windings and $\Delta I_{s,i}$ which circulates between each stator winding (Fig. 4) and described as [16]:

$$I_{si}=I_{s1,i}+I_{s2,i}; \tag{7}$$

$$\Delta I_{s,i}=\frac{I_{s2,i}-I_{s1,i}}{2}. \tag{8}$$

The mean control strategy is based on averaging the input variables of both motors to form a virtual mean motor model. The measured variables for both machines include the stator currents $I_{s1,i}$ and $I_{s2,i}$ and rotor speeds (ω_1, ω_2). The corresponding average quantities are computed as:

$$I_{si}=\frac{I_{s1,i}+I_{s2,i}}{2}; \tag{9}$$

$$\omega_i=\frac{\omega_1+\omega_2}{2}. \tag{10}$$

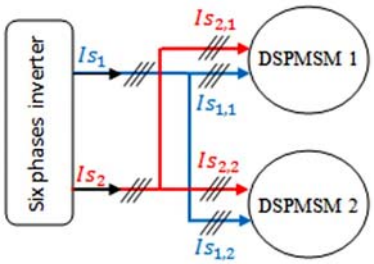

Fig. 4. Current decomposition in the parallel-connected dual motor system

DTC based on fuzzy logic. DTC operates on a fundamental principle that involves selecting appropriate switching commands for the voltage inverter to control the stator voltage vectors. These vectors are carefully chosen from a predefined lookup table based on the estimated torque and flux errors, as well as the angular position of the stator flux vector. Two comparators continuously monitor the key control variables: stator flux and electromagnetic torque.

A hysteresis controller is integrated into the DTC scheme to maintain the error between each control variable and its reference within a defined hysteresis band. In the case of a two-level controller, the voltage vector selection depends solely on the polarity of the error rather than its magnitude. To avoid unnecessary switching when the flux error becomes negligible, a hysteresis band centered around zero is introduced [15].

Fundamentally, DTC relies on the orientation and regulation of the stator flux. The mathematical expression of the stator flux in the Park reference frame is given as:

$$\begin{aligned} \Phi_{ds(1,2)}&=\frac{1}{2}\int_0^t\left(V_{1ds(1,2)}+V_{2ds(1,2)}\right)dt-\\ &-\frac{1}{2}\int_0^t R_s\cdot\left(I_{1ds(1,2)}+I_{2ds(1,2)}\right)dt; \end{aligned} \tag{11}$$

$$\begin{aligned} \Phi_{qs(1,2)}&=\frac{1}{2}\int_0^t\left(V_{1qs(1,2)}+V_{2qs(1,2)}\right)dt-\\ &-\frac{1}{2}\int_0^t R_s\cdot\left(I_{1qs(1,2)}+I_{2qs(1,2)}\right)dt; \end{aligned} \tag{12}$$

Consequently, the stator flux module is:

$$\Phi_{s1}=\sqrt{\Phi_{ds1}^2+\Phi_{qs1}^2}; \tag{13}$$

$$\Phi_{s2}=\sqrt{\Phi_{ds2}^2+\Phi_{qs2}^2}. \tag{14}$$

The electromagnetic torque can be estimated from the estimated magnitudes of the flux, and the measured magnitudes of the line currents:

$$\begin{aligned} T_e=\frac{p}{2}\big[&\Phi_{ds1}\cdot\left(I_{1qs1}+I_{2qs1}\right)-\Phi_{qs1}\cdot\left(I_{1ds1}+I_{2ds1}\right)+\\ &+\Phi_{ds2}\cdot\left(I_{1qs2}+I_{2qs2}\right)-\Phi_{qs2}\cdot\left(I_{2ds2}+I_{2ds2}\right). \end{aligned} \tag{15}$$

To enhance the performance of conventional DTC, particularly by reducing torque and flux ripples and improve the THD of the stator current, the hysteresis controllers and switching table are replaced with fuzzy logic-based decision blocks. These blocks take as inputs the stator flux angle, torque error, and flux error, resulting in a fuzzy logic-based DTC scheme [14, 19, 31].

The universe of discourse for the stator flux angle is divided into 6 fuzzy sets (t_1–t_6) (Fig. 5,*a*). Triangular MFs are used for all angular sectors (t_i). The universe of discourse for the electromagnetic torque error is divided into 3 fuzzy sets (Fig. 5,*b*): Negative torque error (*N*), Zero torque error (*Z*) and Positive torque error (*P*). Triangular MFs are assigned to the central fuzzy set (*Z*), while trapezoidal MFs are used for the boundary sets (*P*) and (*N*).

Similarly, the universe of discourse for the stator flux error is divided into 2 fuzzy sets (Fig. 5,*c*): Negative flux error (*N*), Positive flux error (*P*). For both sets, trapezoidal MFs are selected to better accommodate uncertainties at the boundaries of the domain.

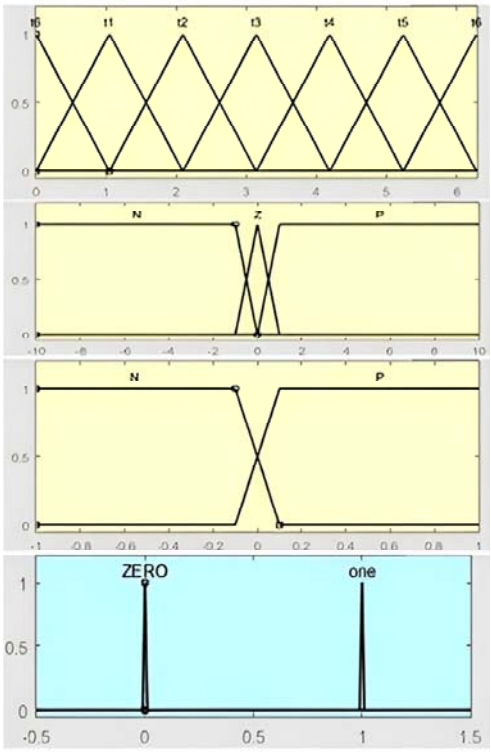

Fig. 5. MFs of the input and output variables used in the fuzzy DTC

The output variable, illustrated in Fig. 5,*d*, is decomposed into 3 sub-outputs, corresponding to the 3 switching signals S_a, S_b, S_c used to control the inverter switches in a two-level configuration. The universe of discourse for each sub-output is divided into 2 fuzzy sets: Zero and One. Trapezoidal MFs are selected for both sets to ensure robust switching decisions under uncertainty.

T2-FLC, which relies on type-2 fuzzy sets (T2-FS), is a powerful approach for managing complex and nonlinear systems [34]. To address higher levels of uncertainty in modelling and control, T2-FS are introduced as an extension of the conventional type-1 fuzzy sets (T1-FS) to better handle uncertainty and imprecision in complex systems [16, 34–36]. Numerous studies have demonstrated that T2-FLC offers superior performance compared to T1-FLC, particularly in environments characterized by high levels of uncertainty and nonlinearity. The fuzzy rule base forms the core of the T2-FLC system. It encapsulates expert knowledge through a set of fuzzy rules that describe the expected behavior of the system under different operating conditions. In this work, the rule base consists of 36 fuzzy rules (Table 1).

Table 1

Set of fuzzy rules

Flux error $\Delta\Phi$	Torque error ΔT_e	Stator flux angle θ					
		t_1	t_2	t_3	t_4	t_5	t_6
P	*P*	*V*3	*V*4	*V*5	*V*6	*V*1	*V*2
	Z	*V*0	*V*7	*V*0	*V*7	*V*0	*V*7
	N	*V*1	*V*2	*V*3	*V*4	*V*5	*V*6
N	*P*	*V*4	*V*5	*V*6	*V*1	*V*2	*V*3
	Z	*V*7	*V*0	*V*7	*V*0	*V*7	*V*0
	N	*V*6	*V*1	*V*2	*V*3	*V*4	*V*5

where:

*V*0= [0 0 0]; *V*1= [1 0 0]; *V*2= [1 1 0]; *V*3= [0 1 0];
*V*4= [0 1 1]; *V*5= [0 0 1]; *V*6= [1 0 1]; *V*7= [1 1 1].

T-2FLC of DSPMSM. This section describes the implementation of T2-FLC, which effectively replaced the PI controller in order to achieve faster response times while maintaining system stability and eliminating static error. T2-FLC is well-suited to handling complex non-linear systems that exhibit a degree of uncertainty [16]. It does not require an exact model of the system or precise parameter values [17].

T2-FLC contains 4 elements [16, 18]:

- **Fuzzification**. This initial step involves the transformation of classical data into MFs such as negative grand (NG), equal zero (EZ) and so on.
- **Fuzzy inference engine**. This component leverages a lookup table that consolidates control derivatives obtained from the interplay of control rules and MFs .
- **Type reducer**. This essential component of the T2-FLC is responsible for transforming the output of T1-FS and subsequently transferring it to the defuzzification process.
- **Defuzzification**. The output from the type reducer is further processed through the defuzzification process, which converts MFs into crisp data.

In this specific application (Fig. 6) the T2-FLC uses 2 input variables: the speed error (e_s) and the variation in speed error (Δe_s). The output variable U_f is generated through the fuzzy inference and defuzzification process, and corresponds to the electromagnetic torque reference T_e.

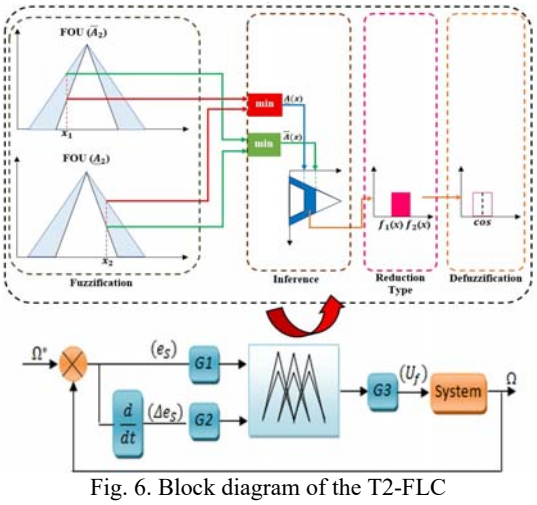

Fig. 6. Block diagram of the T2-FLC

MFs associated with the input variables are depicted in Fig. 7. T2-FLC follows the conventional IF–THEN rule-based structure; however, it differs from classical fuzzy controllers by employing T2-FS for both the antecedents and the consequents [37–39]. T2-FLC represents an innovative and robust control strategy that

offers enhanced flexibility in managing uncertainties and handling complex nonlinear dynamics. By incorporating a footprint of uncertainty (FOU) in its MFs, the T2-FLC has the potential to significantly improve the performance and reliability of control systems operating under imprecise or variable conditions.

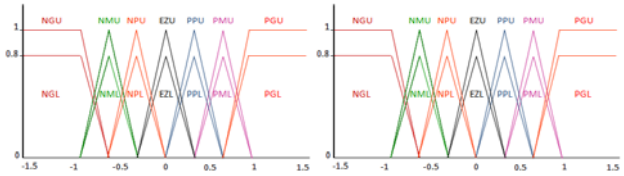

Fig. 7. MFs of the input variables

To illustrate the operation of the proposed T2-FLC for speed control, a few representative fuzzy rules are presented below:

Rule 1: if e_s is NG, and Δe_s is NG then U_f is NG.
Rule 2: if e_s is NG, and Δe_s is NM then U_f is NG.
Rule 3: if e_s is NG, and Δe_s is NP then U_f is NG.
……
Rule 36: if e_s is PG, and Δe_s is PG then U_f is PG.

Simulation results and discussion. The described mathematical model was used to develop the simulation environment in MATLAB/Simulink. The parameters of the DSPMSM were adopted from [14] and are listed in Table 2.

Table 2

Simulation parameters of the DSPMSM

Parameter	Value
Nominal stator voltage U, V	220
Stator resistances $R_{s1} = R_{s2}$, Ω	0.12
Stator inductance L_s, mH	0.8
Mutual inductance L_m, mH	0.3
Flux linkage Φ_{PM}, Wb	0.394
Pole pairs p	4
Moment of inertia J, kg·m^2	$5 \cdot 10^{-5}$
Viscous friction coefficient fr, N·m·s/rad	0
PI controller gain (integral) K_i	3
PI controller gain (proportional) K_p	900
T2-FLC gains G_1, G_2, G_3	0.021
	0.012
	100

The simulation model was developed to enable the performance evaluation of various DTC strategies. To that end, 3 distinct test scenarios were defined for comparative analysis:

Test 1. Speed reversal with load torque steps. This scenario evaluates tracking performance and disturbance rejection capabilities. A trapezoidal reference speed profile alternating between +150 rad/s, –150 rad/s and +50 rad/s was applied. Simultaneously, a load torque of 20 N·m was imposed on both machines.

Test 2. Load torque variation. Designed to assess the dynamic response to external load disturbances, this test involved stepping the load torque from 0 to 20 N·m, then to 40 N·m, and finally back to 20 N·m, while maintaining a constant reference speed of 150 rad/s.

Test 3. Parameter uncertainty. This test focuses on evaluating robustness against internal variations by modelling +100 % increase in the stator resistance R_s.

The proposed T2-FLC was compared via conventional PI-DTC scheme. Performance metrics such as speed tracking accuracy, electromagnetic torque ripple, and robustness to disturbances were recorded for a comprehensive quantitative comparison.

The simulation results clearly indicate that the T2-FLC significantly enhances the control performance of the DSPMSM under all test conditions, particularly in terms of disturbance rejection and reduced torque ripple, outperforming the classical PI-DTC strategy.

Test 1. In the 1st scenario, both motors were subjected to a trapezoidal reference speed profile comprising positive and negative transitions. A load torque of 20 N·m was applied at different time intervals: motor 1 at $t \in [0.1, 0.2]$ and motor 2 at $t \in [0.14, 0.2]$. The simulation results (Fig. 8, 9) provide a detailed view of the system's dynamic behavior, highlighting the effectiveness of the proposed T2-FLC in tracking and disturbance rejection.

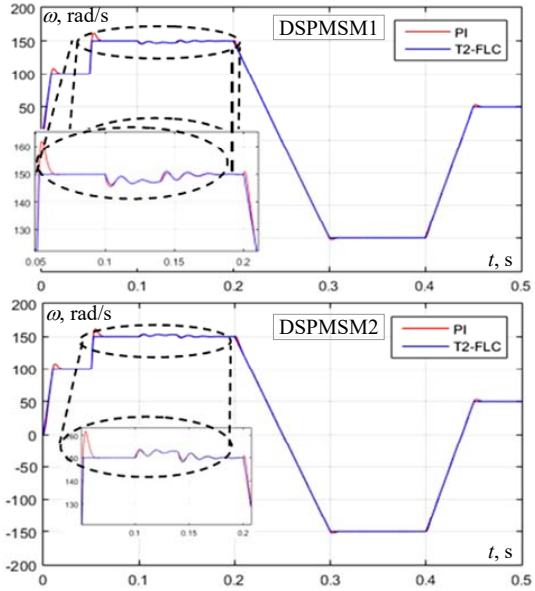

Fig. 8. Speed response of the two DSPMSMs in Test 1

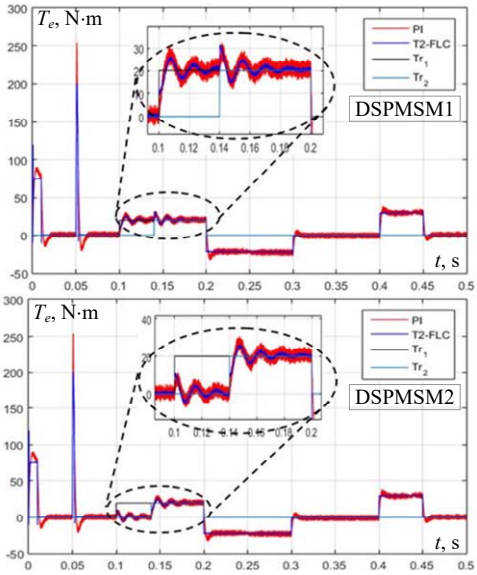

Fig. 9. Torque waveforms of the two DSPMSMs in Test 1

It is evident from the simulation results that the T2-FLC exhibits superior performance in accurately tracking the reference speed trajectory. To facilitate a quantitative comparison between the proposed T2-FLC and the conventional PI-based DTC, several performance indices

have been calculated, including the Integral Squared Error (ISE), Integral Absolute Error (IAE), and Integral Time Squared Error (ITSE) (see Table 3).

T2-FLC successfully tracks a wide speed range, achieving a transition from +150 rad/s to –150 rad/s at t=0.2 s, and reaching 50 rad/s at t=0.4 s. Moreover, the controller demonstrates significantly reduced oscillation amplitudes and enhanced disturbance rejection, confirming its superior dynamic response and robustness compared to the classical PI controller

Test 2. In this scenario, the system's ability to handle external load disturbances was thoroughly evaluated. The load torque applied to the motors was varied in three steps: from 0 N·m to 20 N·m at t=0.12 s, then increased to 40 N·m at t=0.2 s, and finally reduced back to 20 N·m at t=0.28 s. The corresponding simulation results motor speed, electromagnetic torque, and stator currents are illustrated in Fig. 10–12.

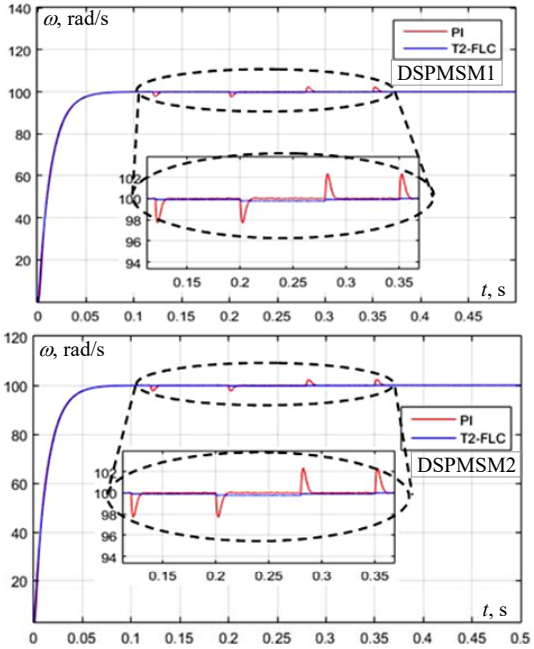

Fig. 10. Speed response of the two DSPMSMs under load torque variation

As shown in Fig. 10, T2-FLC maintained accurate speed regulation across all disturbance intervals, with deviations confined within a narrow margin of ±0.5 rad/s from the reference speed of 150 rad/s. This result underscores the controller's strong capability for disturbance rejection, consistent with findings reported in [9]. In contrast, the PI-based DTC exhibited notable speed deviations, reaching over ±2 rad/s, revealing its limitations in coping with rapid load variations.

The torque waveforms (Fig. 11) further highlight the contrast between the two control strategies. T2-FLC achieved a peak-to-peak torque ripple of only ±3 N·m, demonstrating smoother torque behavior and better dynamic stability. In comparison, the PI controller showed substantial oscillations, with ripple amplitudes reaching ±10 N·m, indicating poorer disturbance rejection and less stable operation. It is important to note that minimizing torque pulsations is critical for precise and efficient operation of PMSMs, particularly in applications requiring high dynamic performance [7].

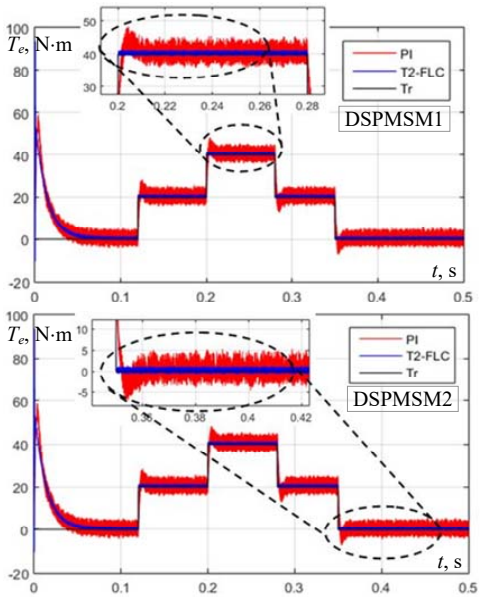

Fig. 11. Comparison of torque ripple under T2-FLC and PI controllers in Test 2

The stator current (Fig. 12) offers additional insight into the performance distinction between the T2-FLC and the PI controller.

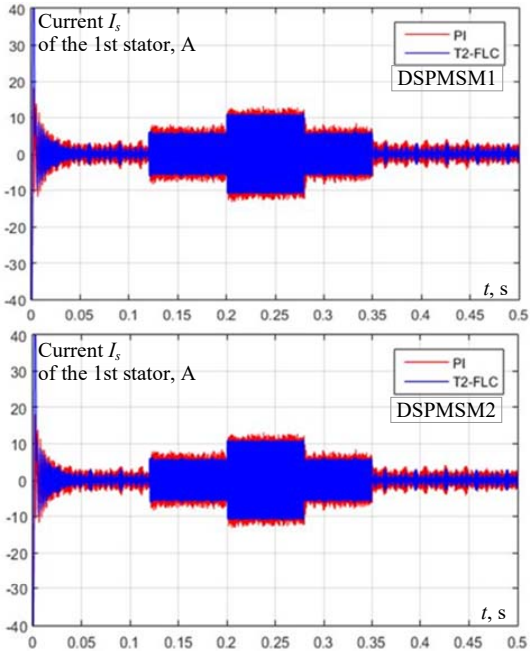

Fig. 12. Stator current response of the two DSPMSMs under load torque variation (Test 2)

Under load variations, the T2-FLC maintains a smooth and nearly circular current trajectory, indicating stable operation and consistent current regulation. In contrast, the PI controller displays noticeable distortions and irregularities in the current locus, along with a slower settling time following torque disturbances, as also noted in [11]. These results confirm the robustness and dynamic stability of the T2-FLC, even under fluctuating load conditions. In summary, the load torque variation test demonstrates that the T2-FLC offers superior disturbance rejection, smoother current dynamics, and faster recovery than the conventional PI-based DTC approach.

Test 3. While the previous tests focused on the response to external disturbances such as speed reversals

and load torque variations, this experiment evaluates the robustness of the control strategy under an internal disturbance. Specifically, a 100 % increase in stator resistance was introduced to simulate parameter uncertainty, which is common in real-world operating conditions due to temperature variation or aging effects. Figure 13 illustrates the speed responses of both DSPMSMs under this condition. The results reveal a clear distinction in performance between the two control approaches. T2-FLC shows strong robustness, maintaining precise speed tracking despite the abrupt internal change. The speed error remains within a narrow tolerance band, indicating effective compensation for the parameter deviation. Figures 13–16 illustrate the impact of these parameter variations on speed, torque, stator current, and stator flux.

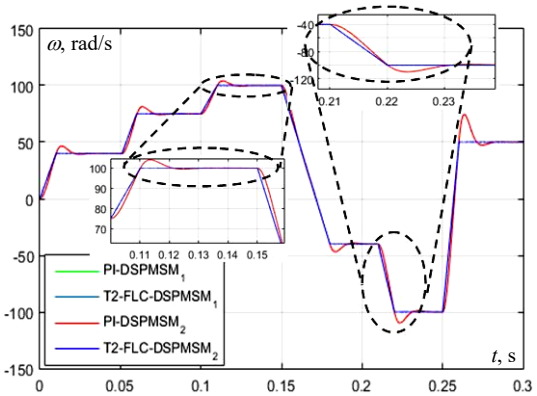

Fig. 13. Speed response of the two DSPMSMs under internal parameter variation (Test 3)

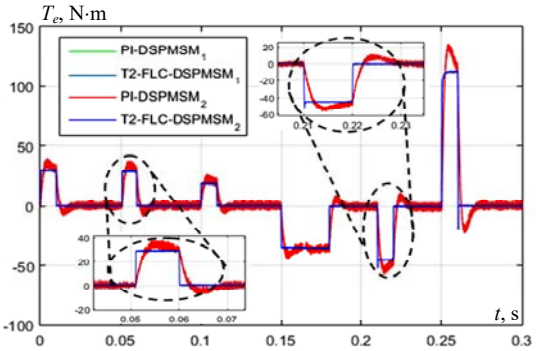

Fig. 14. Torque ripple performance of DSPMSMs under stator resistance variation

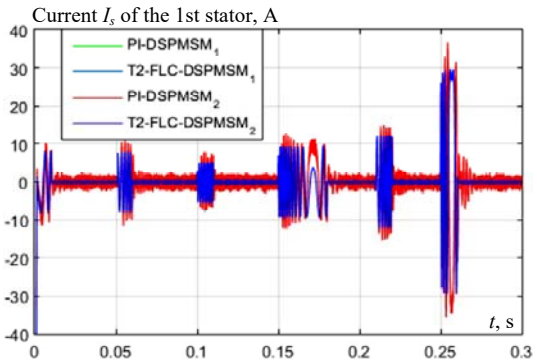

Fig. 15. Stator current response of the two DSPMSMs under internal parameter variation (Test 3)

In contrast, the PI-based DTC exhibits degraded performance, with noticeable speed deviations and slower convergence to the reference trajectory. This confirms the sensitivity of conventional PI control to internal parameter variations, and highlights the adaptive nature of the T2-FLC in uncertain environments.

Overall, this test reinforces the T2-FLC's superior adaptability and resilience in the presence of internal uncertainties, further validating its effectiveness for real-time motor drive applications.

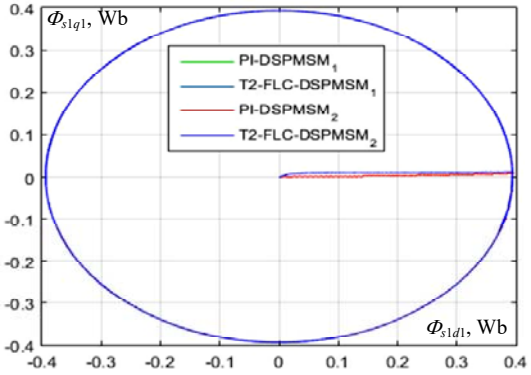

Fig. 16. Comparison of stator flux behavior under internal disturbances (Test 3)

Discussion. The simulation results offer valuable insights into the performance of the T2-FLC for the DSPMSM when compared to the conventional PI controller. This section provides a detailed interpretation of those results, supported by quantitative metrics. Table 3 shows a summary of performance indices ISE, IAE and ITSE across 3 test scenarios. The recorded values clearly validate the simulation outcomes and confirm the effectiveness of the proposed T2-FLC strategy.

Table 3

Comparison of ISE, IAE and ITSE for PI and T2-FLC under different test conditions

	Controller	ISE	IAE	ITSE
Test 1	PI	3.425	0.2889	0.204
	T2-FLC	2.355	0.0982	0.1197
Test 2	PI	0.1892	0.0912	0.01832
	T2-FLC	0.0066	0.0388	0.00139
Test 3	PI	1.738	0.3162	0.387
	T2-FLC	0.0769	0.0401	0.0194

In addition to the error-based indices, dynamic performance was also assessed. As shown in Table 4, the T2-FLC controller outperformed the PI controller across all measured criteria. The settling time was reduced from 0.52 s to 0.28 s, and the overshoot was lowered from 12 % to 7 %. The steady-state error decreased significantly from 0.04 to less than 0.01. Furthermore, under a load disturbance applied at t = 1.5 s, the T2-FLC restored the system stability within 0.12 s, while the PI controller required 0.26 s.

Table 4

Dynamic performance comparison between PI and T2-FLC

Performance metrics	PI	T2-FLC
Settling time, s	0.52	0.28
Overshoot, %	12 %	7 %
Steady-state error	0.04	<0.01
Recovery time after disturbance, s	0.26	0.12

The results consistently demonstrate the superiority, robustness, and adaptability of the proposed control approach. T2-FLC provides improved tracking accuracy, reduced torque ripple, and better disturbance rejection under both external and internal perturbations. These findings confirm that T2-FLC is a reliable and promising

control solution for DSPMSMs, especially in demanding industrial and traction applications.

In the first test, both motors were subjected to a trapezoidal speed profile with a 20 N·m load torque applied. The results in Fig. 8, 9 highlight the superior performance of T2-FLC controller. T2-FLC shown exceptional speed tracking capabilities, efficiently transitioning between positive and negative speed values. Notably, transient speed oscillations were significantly reduced, emphasizing its improved dynamic response compared to the standard PI controller.

The second test assessed the system's response to varying load torque. As seen in Fig. 10, T2-FLC controller consistently maintained precise speed regulation even under fluctuating load conditions, showcasing its robust disturbance rejection capabilities. In contrast, PI controller exhibited greater speed deviations, indicating its inferior ability to reject disturbances. Analysis of torque waveforms (Fig. 11) demonstrated that T2-FLC effectively minimized torque pulsations, a critical factor for the precise control of PMSM. Additionally, the stator current locus plot (Fig. 12) showed that T2-FLC maintained a cleaner and more consistent response, even in the presence of load variations.

The final test evaluated the performance of both controllers under parametric uncertainties, specifically a 100 % increase in stator resistance. PI controller exhibited sensitivity to these disturbances, with noticeable deviations in the system's responses. In contrast, T2-FLC controller displayed resilience and maintained stable performance, highlighting its robustness against internal parameter mismatches.

Overall, the results from these tests suggest that the proposed T2-FLC controller offers significant advantages over the conventional PI controller, particularly in terms of dynamic response, disturbance rejection, and robustness. T2-FLC controller demonstrated precise speed control, reduced torque pulsations, and consistent performance under varying load conditions and internal disturbances. This highlights the potential of T2-FLC to enhance the efficiency and robustness of DSPMSMs in practical applications. While T2-FLC controller shows considerable promise, it is important to acknowledge certain limitations, such as the increased computational complexity. Future work could focus on optimizing the controller for real-time applications, with a particular emphasis on reducing computational overhead and ensuring real-time performance. Additionally, experimental validation in practical settings is essential to confirm the simulation results and further refine the controller for industrial applications.

Conclusions. In this study, an intelligent DTC strategy based on T2-FLC was proposed for the speed regulation of two parallel-connected DSPMSMs powered by a single six-phase inverter. By replacing the conventional PI controller with T2-FLC, the proposed control approach aims to enhance dynamic performance, robustness, and precision in multi-machine drive systems.

Simulation results confirmed that T2-FLC significantly improves tracking accuracy, reduces torque and flux ripples, and enhances the system's ability to reject external disturbances and withstand internal parameter variations. Compared to the conventional PI-based DTC, the proposed method consistently delivered superior dynamic response, better stability, and greater resilience to uncertainties.

These findings demonstrate the potential of T2-FLC-based DTC as a robust and efficient control solution for complex multi-machine architectures, particularly in high-performance applications such as electric traction, marine propulsion, and industrial automation.

Future work will focus on the real-time implementation of the proposed controller and its experimental validation on a physical test bench to further assess its practical applicability and performance in real-world environments. This step is essential to confirm the simulation outcomes and to verify the robustness of T2-FLC under actual operating conditions.

Conflict of interest. The authors declare that they have no conflicts of interest.

REFERENCES

1. Barrero F., Duran M.J. Recent Advances in the Design, Modeling, and Control of Multiphase Machines—Part I. *IEEE Transactions on Industrial Electronics*, 2016, vol. 63, no. 1, pp. 449-458. doi: https://doi.org/10.1109/TIE.2015.2447733.

2. Jones M., Vukosavic S.N., Levi E. Parallel-Connected Multiphase Multidrive Systems With Single Inverter Supply. *IEEE Transactions on Industrial Electronics*, 2009, vol. 56, no. 6, pp. 2047-2057. doi: https://doi.org/10.1109/TIE.2009.2017219.

3. Parsa L. On advantages of multi-phase machines. *31st Annual Conference of IEEE Industrial Electronics Society, 2005. IECON 2005*, 6 p. doi: https://doi.org/10.1109/IECON.2005.1569139.

4. Demir Y., Aydin M. A Novel Dual Three-Phase Permanent Magnet Synchronous Motor With Asymmetric Stator Winding. *IEEE Transactions on Magnetics*, 2016, vol. 52, no. 7, pp. 1-5. doi: https://doi.org/10.1109/TMAG.2016.2524027.

5. Kozovsky M., Blaha P. Double three-phase PMSM structures for fail operational control. *IFAC-PapersOnLine*, 2019, vol. 52, no. 27, pp. 1-6. doi: https://doi.org/10.1016/j.ifacol.2019.12.733.

6. Vu D.T., Nguyen N.K., Semail E., Nguyen T.T.N. Current Harmonic Eliminations for Seven-Phase Non-sinusoidal PMSM Drives applying Artificial Neurons. *Lecture Notes in Networks and Systems*, 2021, vol. 178, pp. 270–279. doi: https://doi.org/10.1007/978-3-030-64719-3_31.

7. Nguyen N.L., Fadel M., Llor A. A new approach to Predictive Torque Control with Dual Parallel PMSM system. *2013 IEEE International Conference on Industrial Technology (ICIT)*, 2013, pp. 1806-1811. doi: https://doi.org/10.1109/ICIT.2013.6505950.

8. Wang X., Yan H., Sala G., Buticchi G., Gu C., Zhao W., Xu L., Zhang H. Selective Torque Harmonic Elimination for Dual Three-Phase PMSMs Based on PWM Carrier Phase Shift. *IEEE Transactions on Power Electronics*, 2020, vol. 35, no. 12, pp. 13255-13269. doi: https://doi.org/10.1109/TPEL.2020.2991264.

9. Anka Rao M., Vijayakumar M., Kumar N.P. Speed control of parallel connected DSIM fed by six phase inverter with IFOC strategy using ANFIS. *International Journal of Research and Engineering*, 2017, vol. 4, no. 9, pp. 244-249.

10. Lee Y., Ha J.-I. Control Method for Mono Inverter Dual Parallel Surface-Mounted Permanent-Magnet Synchronous Machine Drive System. *IEEE Transactions on Industrial Electronics*, 2015, vol. 62, no. 10, pp. 6096-6107. doi: https://doi.org/10.1109/TIE.2015.2420634.

11. Ramachandran G., Veerana S., Padmanaban S. Vector control of a three-phase parallel connected two motor single inverter speed sensorless drive. *Turkish Journal of Electrical Engineering & Computer Sciences*, 2016, vol. 24, pp. 4027-4041. doi: https://doi.org/10.3906/elk-1410-48.

12. Wang Z., Wang X., Cao J., Cheng M., Hu Y. Direct Torque Control of T-NPC Inverters-Fed Double-Stator-Winding PMSM Drives With SVM. *IEEE Transactions on Power Electronics*, 2018, vol. 33, no. 2, pp. 1541-1553. doi: https://doi.org/10.1109/TPEL.2017.2689008.

13. Kamel T., Abdelkader D., Said B., Padmanaban S., Iqbal A. Extended Kalman Filter Based Sliding Mode Control of Parallel-Connected Two Five-Phase PMSM Drive System. *Electronics*, 2018, vol. 7, no. 2, art. no. 14. doi: https://doi.org/10.3390/electronics7020014.

14. Laggoun L., Kiyyour B., Boukhalfa G., Belkacem S., Benaggoune S. Direct Torque Control Using Fuzzy Second Order Sliding Mode Speed Regulator of Double Star Permanent Magnet Synchronous Machine. *Lecture Notes in Electrical Engineering*, 2021, vol. 682, pp. 139-153. doi: https://doi.org/10.1007/978-981-15-6403-1_10.
15. Tir Z., Malik O.P., Eltamaly A.M. Fuzzy logic based speed control of indirect field oriented controlled double star induction motors connected in parallel to a single six-phase inverter supply. *Electric Power Systems Research*, 2016, vol. 134, pp. 126-133. doi: https://doi.org/10.1016/j.epsr.2016.01.013.
16. Bounab A., Chaiba A., Belkacem S. Evaluation of the High Performance Indirect Field Oriented Controlled Dual Induction Motor Drive Fed by a Single Inverter using Type-2 Fuzzy Logic Control. *Engineering, Technology & Applied Science Research*, 2020, vol. 10, no. 5, pp. 6301-6308. doi: https://doi.org/10.48084/etasr.3799.
17. Liang Q., Mendel J.M. Interval type-2 fuzzy logic systems: theory and design. *IEEE Transactions on Fuzzy Systems*, 2000, vol. 8, no. 5, pp. 535-550. doi: https://doi.org/10.1109/91.873577.
18. Mehedi F., Yahdou A., Djilali A., Benbouhenni H. Direct Torque Fuzzy Controlled Drive for Multi-phase IPMSM Based on SVM Technique. *Journal Europeen des Systemes Automatises*, 2020, vol. 53, no. 2, pp. 259-266. doi: https://doi.org/10.18280/jesa.530213.
19. Mehedi F., Nezli L., Mahmoudi M.O.H., Taleb R., Boudana D. Fuzzy logic based vector control of multi-phase permanent magnet synchronous motors. *Journal of Renewable Energies*, 2023, vol. 22, no. 1, pp. 161-170. doi: https://doi.org/10.54966/jreen.v22i1.734.
20. Bai Y., Wang D. On the Comparison of Type 1 and Interval Type 2 Fuzzy Logic Controllers Used in a Laser Tracking System. *IFAC-PapersOnLine*, 2018, vol. 51, no. 11, pp. 1548-1553. doi: https://doi.org/10.1016/j.ifacol.2018.08.276.
21. Karnik N.N., Mendel J.M. Operations on type-2 fuzzy sets. *Fuzzy Sets and Systems*, 2001, vol. 122, no. 2, pp. 327-348. doi: https://doi.org/10.1016/S0165-0114(00)00079-8.
22. Sedaghati A., Pariz N., Siahi M., Barzamini R. A new fractional-order developed type-2 fuzzy control for a class of nonlinear systems. *International Journal of Systems Science*, 2023, vol. 54, no. 15, pp. 2840-2858. doi: https://doi.org/10.1080/00207721.2020.1867927.
23. Fouad B., Ali C., Samir Z., Salah S. Direct Torque Control of Induction Motor Fed by Three-level Inverter Using Fuzzy Logic. *Advances in Modelling and Analysis C*, 2017, vol. 72, no. 4, pp. 248-265. doi: https://doi.org/10.18280/ama_c.720404.
24. Venkataramana Naik N., Panda A., Singh S.P. A Three-Level Fuzzy-2 DTC of Induction Motor Drive Using SVPWM. *IEEE Transactions on Industrial Electronics*, 2016, vol. 63, no. 3, pp. 1467-1479. doi: https://doi.org/10.1109/TIE.2015.2504551.
25. Kamalapur G., Aspalli M.S. Direct torque control and dynamic performance of induction motor using fractional order fuzzy logic controller. *International Journal of Electrical and Computer Engineering*, 2023, vol. 13, no. 4, pp. 3805-3816. doi: https://doi.org/10.11591/ijece.v13i4.pp3805-3816.
26. Moussaoui L. Performance enhancement of direct torque control induction motor drive using space vector modulation strategy. *Electrical Engineering & Electromechanics*, 2022, no. 1, pp. 29-37. doi: https://doi.org/10.20998/2074-272X.2022.1.04.
27. Lokriti A., Zidani Y., Doubabi S. Fuzzy logic control contribution to the direct torque and flux control of an induction machine. *2011 International Conference on Multimedia Computing and Systems*, 2011, pp. 1-6. doi: https://doi.org/10.1109/ICMCS.2011.5945645.
28. Boudana D., Nezli L., Tlemçani A., Mahmoudi M., Tadjine M. Robust DTC Based on Adaptive Fuzzy Control of Double Star Synchronous Machine Drive with Fixed Switching Frequency. *Journal of Electrical Engineering*, 2012, vol. 63, no. 3, pp. 133-143. doi: https://doi.org/10.2478/v10187-012-0021-y.
29. Hannan M.A., Ghani Z.A., Mohamed A., Uddin M.N. Real-time testing of a fuzzy logic controller based grid-connected photovoltaic inverter system. *2014 IEEE Industry Application Society Annual Meeting*, 2014, pp. 1-8. doi: https://doi.org/10.1109/IAS.2014.6978394.
30. Kakouche K., Guendouz W., Rekioua T., Mezani S., Lubin T. Application of Fuzzy Controller to Minimize Torque and Flux Ripples of PMSM. *2019 International Conference on Advanced Electrical Engineering (ICAEE)*, 2019, pp. 1-6. doi: https://doi.org/10.1109/ICAEE47123.2019.9015066.
31. Naas B., Nezli L., Naas B., Mahmoudi M.O., Elbar M. Direct Torque Control Based Three Level Inverter-fed Double Star Permanent Magnet Synchronous Machine. *Energy Procedia*, 2012, vol. 18, pp. 521-530. doi: https://doi.org/10.1016/j.egypro.2012.05.063.
32. Guezi A., Bendaikha A., Dendouga A. Direct torque control based on second order sliding mode controller for three-level inverter-fed permanent magnet synchronous motor: comparative study. *Electrical Engineering & Electromechanics*, 2022, no. 5, pp. 10-13. doi: https://doi.org/10.20998/2074-272X.2022.5.02.
33. Lallouani H., Saad B., Letfi B. DTC-SVM based on Interval Type-2 Fuzzy Logic Controller of Double Stator Induction Machine fed by Six-Phase Inverter. *International Journal of Image, Graphics and Signal Processing*, 2019, vol. 11, no. 7, pp. 48-57. doi: https://doi.org/10.5815/ijigsp.2019.07.04.
34. Srinivas G., Durga Sukumar G., Subbarao M. Total harmonic distortion analysis of inverter fed induction motor drive using neuro fuzzy type-1 and neuro fuzzy type-2 controllers. *Electrical Engineering & Electromechanics*, 2024, no. 1, pp. 10-16. doi: https://doi.org/10.20998/2074-272X.2024.1.02.
35. Khemis A., Boutabba T., Drid S. Model reference adaptive system speed estimator based on type-1 and type-2 fuzzy logic sensorless control of electrical vehicle with electrical differential. *Electrical Engineering & Electromechanics*, 2023, no. 4, pp. 19-25. doi: https://doi.org/10.20998/2074-272X.2023.4.03.
36. Rahali H., Zeghlache S., Cherif B.D.E., Benyettou L., Djerioui A. Robust adaptive fuzzy type-2 fast terminal sliding mode control of robot manipulators in attendance of actuator faults and payload variation. *Electrical Engineering & Electromechanics*, 2025, no. 1, pp. 31-38. doi: https://doi.org/10.20998/2074-272X.2025.1.05.
37. Kaddache M., Drid S., Khemis A., Rahem D., Chrifi-Alaoui L. Maximum power point tracking improvement using type-2 fuzzy controller for wind system based on the double fed induction generator. *Electrical Engineering & Electromechanics*, 2024, no. 2, pp. 61-66. doi: https://doi.org/10.20998/2074-272X.2024.2.09.
38. Loukal K., Benalia L. Type-2 Fuzzy Logic Controller of a Doubly Fed Induction Machine. *Advances in Fuzzy Systems*, 2016, vol. 2016, art. no. 8273019. doi: https://doi.org/10.1155/2016/8273019.
39. Rahali H., Zeghlache S., Benalia L. Adaptive Field-Oriented Control Using Supervisory Type-2 Fuzzy Control for Dual Star Induction Machine. *International Journal of Intelligent Engineering and Systems*, 2017, vol. 10, no. 4, pp. 28-40. doi: https://doi.org/10.22266/ijies2017.0831.04.

Received 18.06.2025
Accepted 20.09.2025
Published 02.01.2026

A. Bounab[1]*, PhD Student,*
A. Chaiba[1]*, Professor,*
S. Belkacem[1]*, Professor,*
A. Chariete[2]*, Doctor of Technical Science,*
[1] Department of Electrical Engineering,
University of Batna2, Algeria,
e-mail: bounab_alaeddine@yahoo.fr (Corresponding Author).
[2] Energy and Information Technology Hub,
University of Technology of Belfort-Montbéliard, France.

How to cite this article:
Bounab A., Chaiba A., Belkacem S., Chariete A. Performance improvement of parallel dual-star permanent magnet synchronous machines via type-2 fuzzy direct torque control with a single six-phase inverter. *Electrical Engineering & Electromechanics*, 2026, no. 1, pp. 28-37. doi: https://doi.org/10.20998/2074-272X.2026.1.04